Scott W. Atlas, MD • Alexander S. Mark, MD • Evan K. Fram, MD • Robert I. Grossman, MD

Vascular Intracranial Lesions: Applications of Gradient-Echo MR Imaging[1]

To investigate the role of the gradient-echo (GRE) technique in clinical intracranial magnetic resonance (MR) imaging, 63 patients with a variety of vascular intracranial lesions were examined at 1.5 T with the use of spin-echo (SE) and GRE sequences. In all cases, the sequential section acquisition technique called gradient recalled acquisition in the steady state (GRASS) was employed; a repetition time of 150-200 msec, an echo time of 13-16 msec, and a flip angle of 50°-60° were used to optimize the depiction of blood flow as high intensity and the depiction of stationary fluid as low intensity. In 61 of 63 cases, gradient moment nulling was utilized to compensate for first-order flow effects. Although GRE images rapidly demonstrated flow in vascular intracranial lesions as high intensity, the vascular nature of these lesions was also clearly evident on SE images in most cases. In some cases, GRE images can be used to clarify the vascular nature of a lesion or to characterize a neoplasm. Other applications include the detection of vascular thrombosis, occult vascular malformations, and hemorrhagic complications of vascular lesions.

Index terms: Aneurysm, intracranial, 17.73 • Arteriovenous malformations, cranial, 17.70 • Brain neoplasms, MR studies, 10.36 • Cerebral blood vessels, abnormalities, 17.70 • Cerebral blood vessels, MR studies, 17.1214 • Magnetic resonance (MR), pulse sequences

Radiology 1988; 169:455-461

[1] From the Department of Radiology, Hospital of the University of Pennsylvania, 3400 Spruce St, Philadelphia, PA 19104 (S.W.A., R.I.G.), and the Department of Radiology, University of California at San Francisco (A.S.M., E.K.F.). From the 1987 RSNA annual meeting. Received April 13, 1988; revision requested May 18; revision received June 1; accepted June 27. **Address reprint requests to** S.W.A.

See also the article by Atlas et al (pp 449-453) and the editorial by Bradley (pp 574-575) in this issue.

MAGNETIC resonance (MR) imaging can rapidly depict intravascular flow as high signal intensity when sequential section acquisition and gradient refocusing for echo formation are used (1,2). However, the role of this technique in clinical neurologic imaging has not yet been determined. The purpose of this study was to evaluate and define the clinical applications and possible limitations of gradient-echo (GRE) MR imaging in vascular intracranial lesions.

PATIENTS AND METHODS

Sixty-three patients, aged 11 weeks to 80 years, were examined with MR imaging at 1.5 T (Signa; General Electric Medical Systems, Milwaukee). In all patients, both spin-echo (SE) and GRE images were obtained. Images with a short repetition time (TR) of 500–800 msec and a short echo time (TE) of 20 msec (TR/TE = 500–800/20) were obtained in all cases, as were long TR/short TE (2,500–3,000/20–30) and long TR/TE (2,500–3,000/80) sequences. For 42 of 63 long TR SE images, first-order gradient moment nulling was employed for constant-velocity-flow compensation (3), which has been our standard head imaging protocol since it became available. In all 63 cases, the sequential section acquisition technique called gradient recalled acquisition in the steady state (GRASS) (2) was employed, with a TR of 150–200 msec, a TE of 13–16 msec, and a flip angle of 50°–60°. These imaging variables were selected to optimize the depiction of blood flow as high intensity and the depiction of cerebrospinal fluid and stationary fluid as low intensity (1,2,4,5). In 61 of 63 cases, GRE imaging was performed with first-order gradient moment nulling; in the other two cases, GRE images were obtained without this flow-compensation technique. SE and GRE images were obtained with the use of two to four excitations, a 3–5-mm section thickness, a 0–2.5-mm intersection gap, a 256 × 128 or 256 × 256 matrix, and a 20-cm field of view.

The diagnosis was arteriovenous malformation (AVM) in 23 cases, occult cerebrovascular malformation (cavernous hemangioma) in 11 cases, intracranial neoplasm in seven cases, aneurysm in five cases, venous angioma in five cases, and vessel invasion, occlusion, or thrombosis in 12 cases. These diagnoses were based on surgical and pathologic findings in 17 cases, on angiographic findings in 30 cases, and on a combination of computed tomographic (CT), SE MR, and clinical findings in 16 cases. The SE MR images were compared with the GRE MR images in a retrospective, nonblinded fashion.

RESULTS

Arteriovenous Malformation

In 21 of 23 cases of AVM, the lesions were clearly depicted by both SE and GRE imaging (Fig 1). In the other two cases, the GRE images were superior in defining flow in residual patent vessels after surgery or proton-beam therapy (Fig 2). In all 23 AVMs, the SE findings consisted of serpentine and round areas of signal void (Fig 1). The GRE images varied in their depiction of these lesions. In 14 of 23 cases, the entire AVM, as seen on SE images, was depicted as high intensity on GRE images (Fig 1). In seven of 23 cases, large areas of the lesions depicted as signal void on SE images were also seen as signal void on GRE images obtained with gradient moment nulling (Fig 3). In one AVM, a substantial portion of the lesion was obscured by magnetic susceptibility–related hypointensity artifacts due to its subfrontal location near the interface between the brain and the posterior ethmoid sinus (Fig 4). In one AVM, low intensity was seen in most of the lesion, presumably because no flow-compensation gradients were employed; in this case, the same regions were high intensity on GRE images obtained with the use of gradient moment nulling (Fig 5). In six AVMs, the GRE images were superior in depicting associated hemorrhage, seen as regions of marked hypointensity (Fig 6).

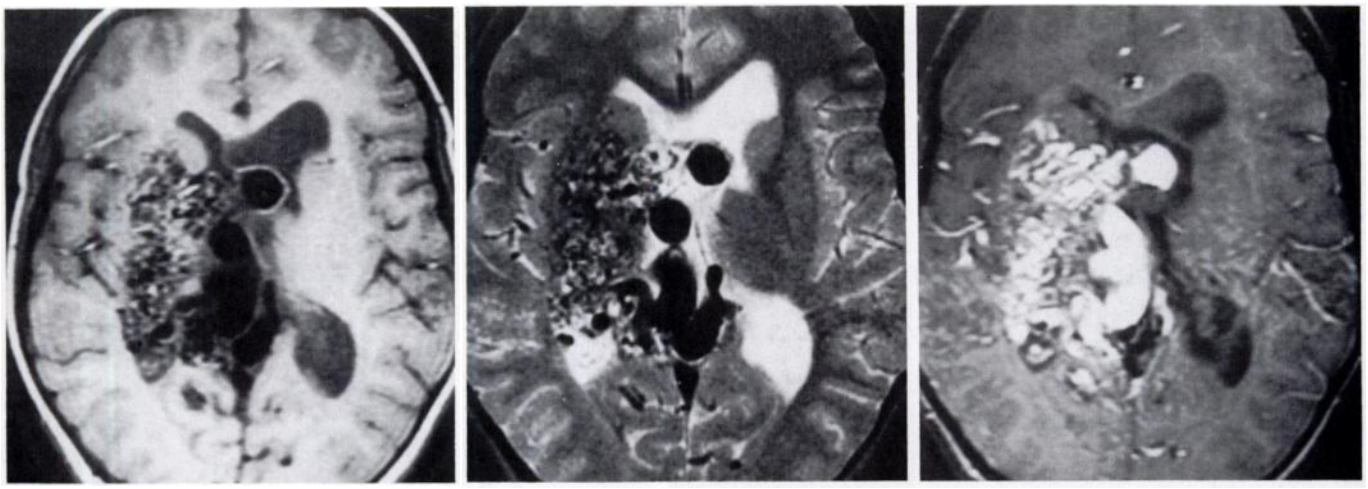

a. b. c.

Figure 1. MR images of AVM with ganglionic and intraventricular components. Large right ganglionic and intraventricular AVM is unambiguously depicted as round and serpentine regions of signal void on axial short TR/TE (600/20) **(a)** and long TR/TE (2,800/80) **(b)** SE images. **(c)** Axial GRE (150/15) image obtained with 50° flip angle demonstrates high intensity in areas of flow depicted as signal void on SE images.

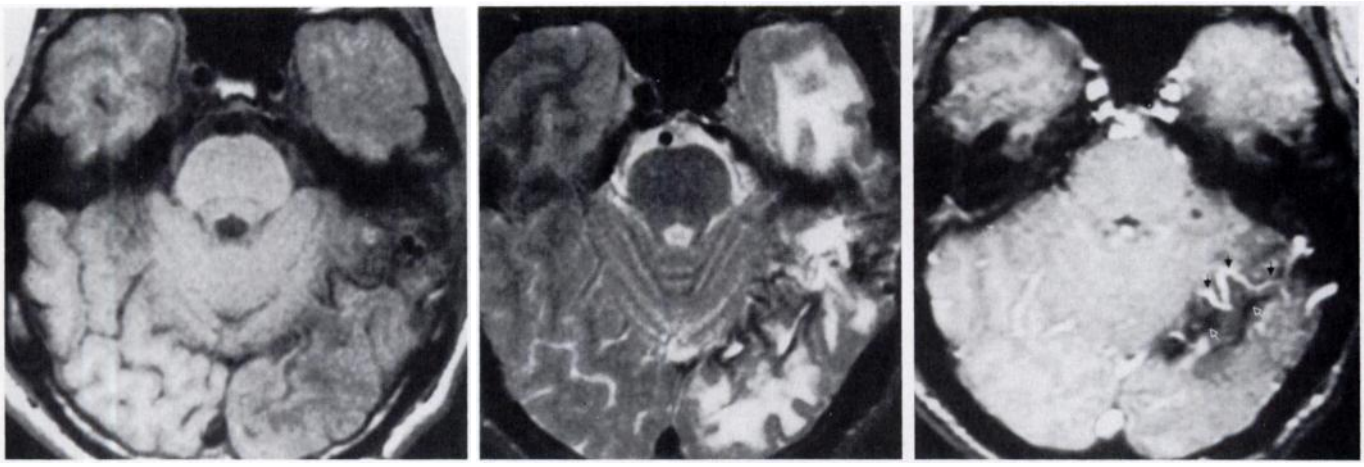

a. b. c.

Figure 2. MR images of residual AVM after proton-beam therapy. Axial short TR/TE (600/20) **(a)** and long TR/TE (2,800/80) **(b)** SE images demonstrate linear areas of hypointensity within larger regions of edema or encephalomalacia in left occipital lobe. **(c)** Confident distinction between hemosiderin from prior hemorrhage (open arrows) and residual patent vessel (closed arrows) can be made only on axial GRE (150/15) image obtained with 50° flip angle.

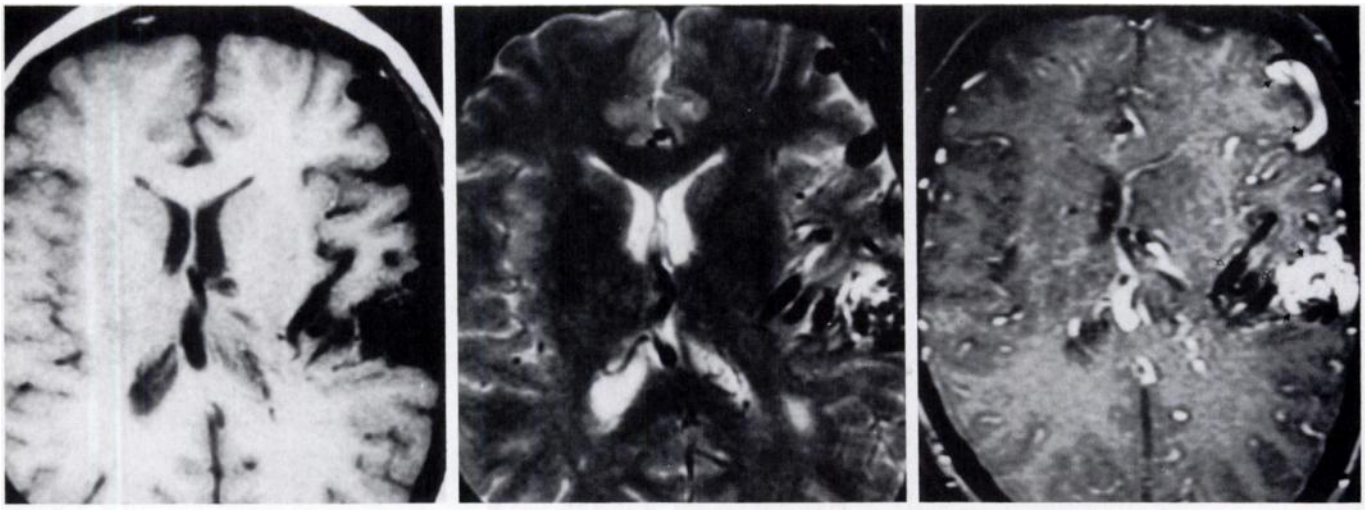

a. b. c.

Figure 3. MR images of left insular and left frontal AVM with turbulent flow. Axial short TR/TE (600/20) **(a)** and long TR/TE (2,800/80) **(b)** SE images clearly depict AVM as signal void. **(c)** Although axial GRE (150/15) image obtained with 50° flip angle depicts some areas of the lesion as high intensity (closed arrows), large regions of patency remain as signal void (open arrows), even though gradient moment nulling was employed. Persistence of signal void was presumably due to turbulence, although uncompensated higher-order flow motion effects may also have contributed to this appearance.

Occult Cerebrovascular Malformation

In four of the 11 cases of occult cerebrovascular malformation, all internal signal characteristics seen on SE images were lost on the GRE images (ie, marked hypointensity was present throughout the lesion) (Fig 7). In nine cases, no evidence of flowing blood within the lesion was seen on GRE images. In two cases, high intensity was present within the lesion on the GRE images, which did not differentiate flow from high-intensity clot. In two cases, additional hypointense lesions were identified on GRE images, which were not clearly seen on SE images; these lesions presumably represented other occult cerebrovascular malformations.

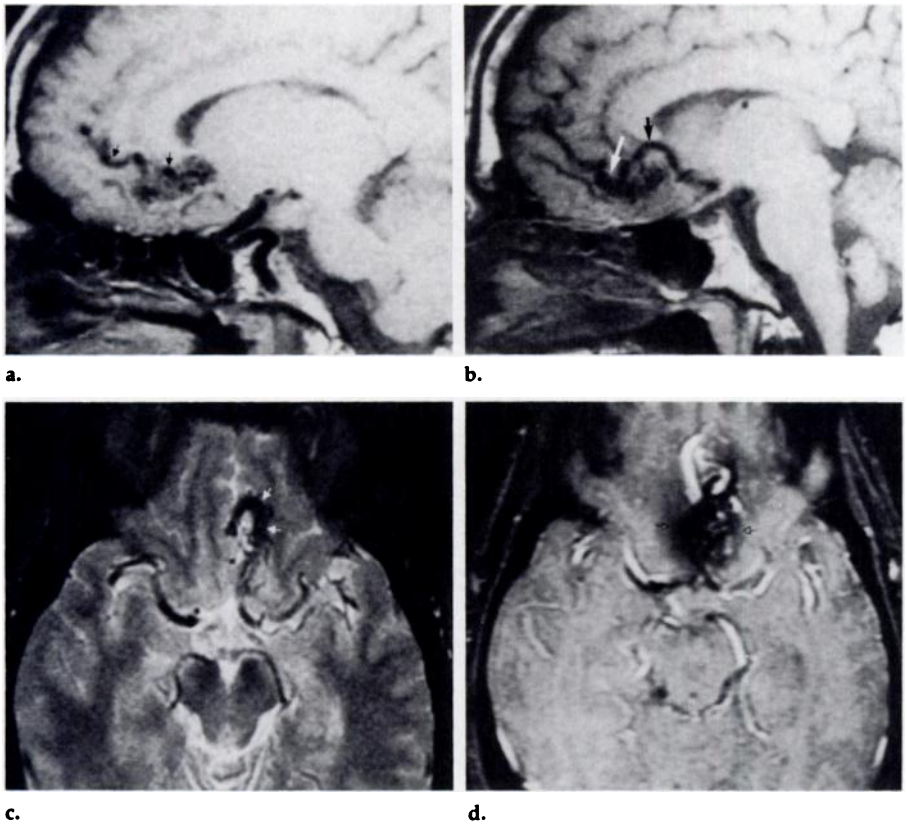

Figure 4. MR images of subfrontal AVM. Sagittal short TR/TE (600/20) **(a, b)** and axial long TR/TE (2,800/80) **(c)** SE images clearly depict subfrontal AVM as regions of signal void (closed arrows). **(d)** On axial GRE (150/15) image obtained with 50° flip angle, portions of the lesion are obscured by hypointensity (open arrows) due to diamagnetic susceptibility gradient-induced signal loss from nearby air-brain interface.

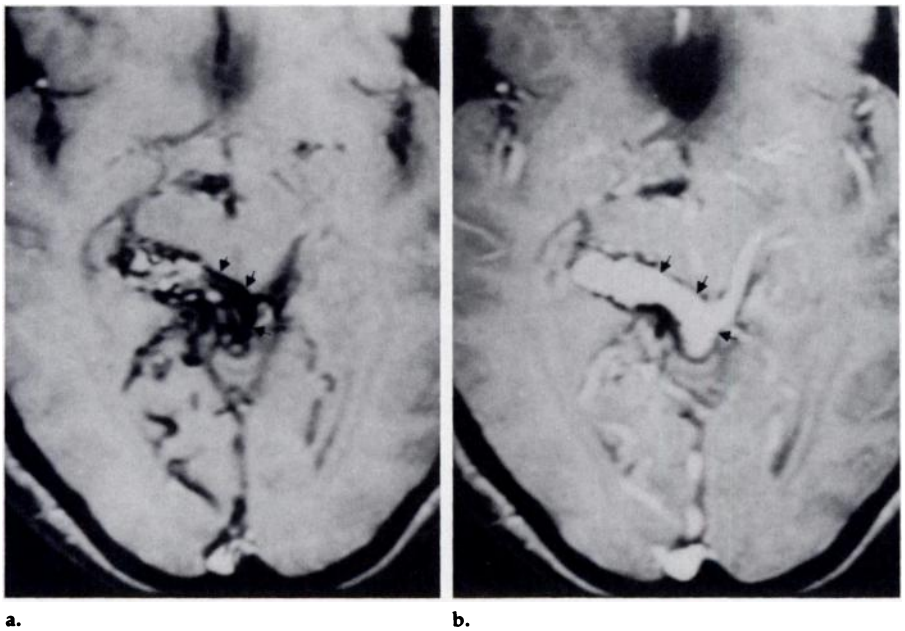

Figure 5. Axial GRE (150/15) images obtained with 50° flip angle. Enlarged vessel draining AVM (arrows) appears as low intensity on image obtained without gradient moment nulling **(a)**, even though sequential section acquisition gradient refocusing was used. High intensity is seen within this vessel on image obtained with gradient moment nulling **(b)**.

Venous Angioma

In three of the five patients with venous angiomas, the GRE images more clearly and more specifically defined the nature of the lesion, when compared with the SE images (Fig 8). In two cases, no additional information was obtained from the GRE images.

Aneurysm

In one of the five patients with aneurysms, the patent portion of the lumen was more clearly identifiable on the GRE image. In two cases, high intensity was present on the GRE images in the thrombosed and patent portions of the aneurysm lumen, thereby making it virtually impossible to distinguish a high-intensity clot from blood flow on the GRE sequence alone (Fig 9). In two cases, there was no difference in diagnostic information obtained with the two imaging techniques.

Neoplasm

In three of the seven cases in which there was a neoplasm, the GRE images were more specific than the SE images in delineating the presence of large intratumoral vessels. In one of these cases, linear and focal areas of signal void on SE images were thought to represent large intratumoral vessels rather than calcification on the basis of morphologic characteristics, but GRE images showed even more profound hypointensity in these areas, indicating magnetic susceptibility-induced signal loss (Fig 10). These areas were found to represent calcification in an ependymoma at CT and surgery. In another patient with a posterior fossa mass thought to be a vascular hemangioblastoma on the basis of CT findings, the SE images demonstrated heterogeneous linear low intensity within the mass, which was suggestive of vessels. GRE images failed to

show high intensity in these areas, and an avascular astrocytoma was found at surgery (Fig 11).

Vessel Patency

In three of the 12 patients examined for patency of vessels at the base of the skull, GRE MR imaging clarified the presence of thrombosis (Figs 12, 13). In two cases, large-vessel displacement and compression by mass lesions were more clearly seen on GRE images. In two cases, high intensity was present in clotted vessels, which appeared as high intensity on SE images, thereby making flow indistinguishable from clot on the basis of GRE imaging alone. In five cases, no additional information was provided by the GRE sequence.

DISCUSSION

Rapid MR imaging utilizing limited flip angles and gradient reversal for echo acquisition can demonstrate blood flow as high signal intensity when the appropriate imaging variables are used (1,2,4,5). The basis of the depiction of moving spins as high intensity on GRE images, as opposed to the signal void seen on SE images, lies in three important features of GRE imaging:

1. With the use of sequential section acquisition rather than an interleaved multisection technique, there is inflow of unsaturated spins into every section (assuming that at least some component of flow is present along the section-select gradient). As a result, each section is like an "entry section"—that is, flow-related enhancement (6,7) is observed on every section in the acquisition (as long as the TR is long enough to avoid steady-state effects). In the non-steady-state situation, the difference between the signal intensity of inflowing spins and that of stationary spins is, to a great extent, related to the flip angle—the larger the flip angle, the greater the difference in signal intensities (1,2,5).

2. The nonselectivity of the refocusing mechanism with GRE imaging is also a factor. In conventional SE imaging, signal void from rapid flow can be at least partially ascribed to movement of spins out of the section between the excitation and refocusing pulses, both of which are section-selective (6,7). To emit a signal in SE imaging, both pulses must be experienced by the spin. In GRE imaging, the refocusing mechanism (in this case, reversal of the read-out gradi-

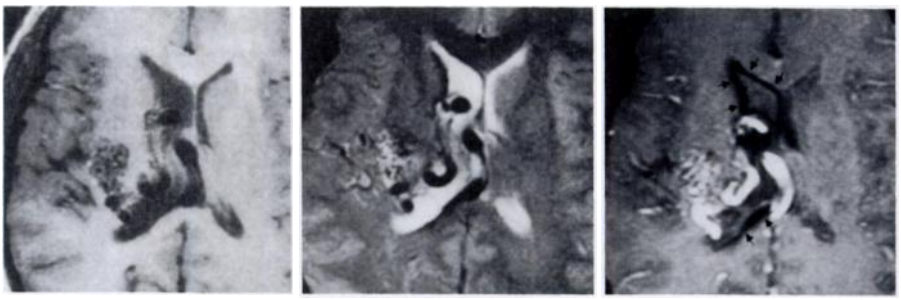

a. b. c.

Figure 6. MR images of intraventricular siderosis from prior hemorrhage and intraventricular AVM. Intraventricular AVM is clearly seen as signal void on axial short TR/TE (600/20) **(a)** and long TR/TE (2,800/80) **(b)** SE images. **(c)** AVM is depicted as high intensity on axial GRE (150/15) image obtained with 50° flip angle. Marked hypointensity lining right ventricle (arrows), more obvious on GRE image, indicates prior intraventricular hemorrhage.

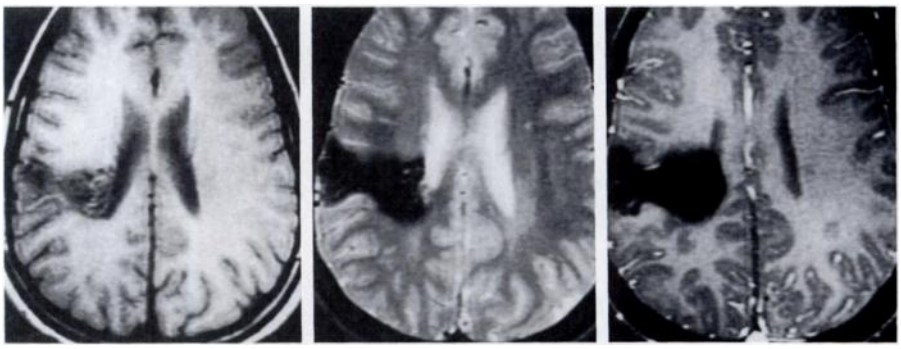

a. b. c.

Figure 7. MR images of right parietal occult cerebrovascular malformation. Focal high-intensity regions are depicted within areas of hemosiderin-related hypointensity on axial short TR/TE (600/20) **(a)** and long TR/TE (2,500/80) **(b)** SE images. **(c)** Axial GRE (150/15) image obtained with 50° flip angle depicts the lesion entirely as an area of hypointensity with no evidence of intralesional flow and without internal signal characteristics.

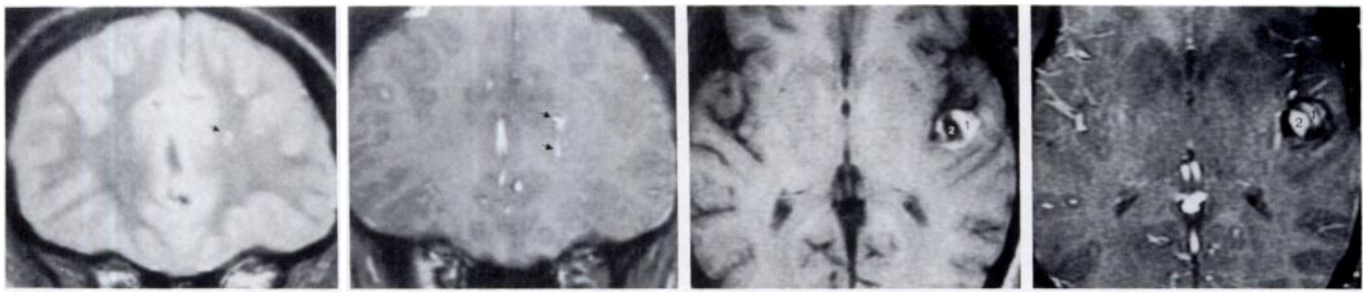

8a. 8b. 9a. 9b.

Figures 8, 9. **(8)** MR images of subtle venous angioma. **(a)** Coronal long TR/short TE (2,800/30) SE image obtained with use of gradient moment nulling depicts lesion as area of slight hyperintensity due to misregistration of compensated flow (arrow) in left frontal deep white matter. **(b)** Coronal GRE (150/15) image obtained with 50° flip angle demonstrates more obvious and more extensive hyperintensity (arrows) in angioma, unambiguously indicating flow. **(9)** MR images of partially thrombosed left middle cerebral artery giant aneurysm depict both thrombosed (*1*) and patent (*2*) portions of lumen. **(a)** On axial short TR/TE (600/20) SE image, thrombosed portion of lumen appears as high intensity, clearly distinguishable from patent portion of lumen, which is seen as signal void. **(b)** Axial GRE (150/15) image obtained with 50° flip angle depicts both portions of the lumen as areas of high intensity.

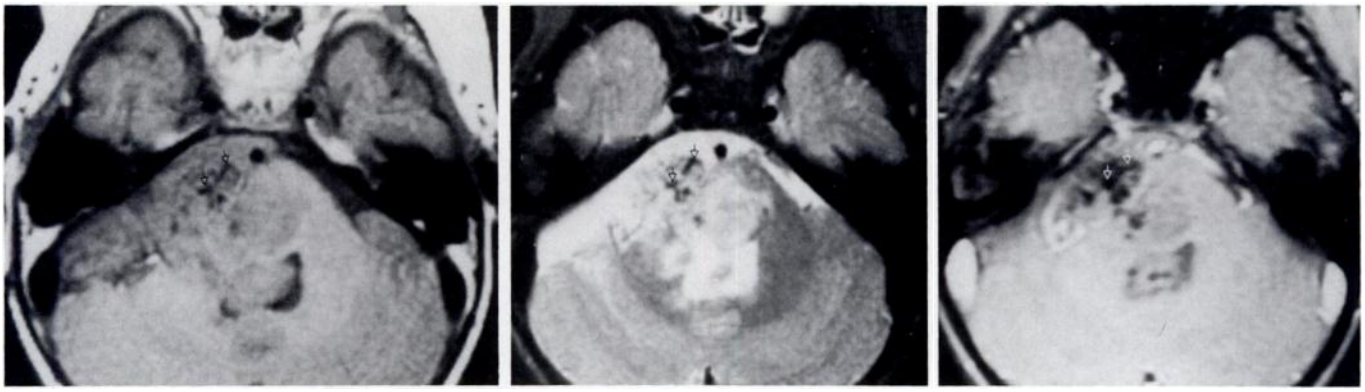

a. b. c.

Figure 10. MR images depicting calcification in ependymoma. Right cerebellopontine angle mass contains linear and focal regions of signal void (arrows) on axial short TR/TE (600/20) **(a)** and long TR/TE (2,800/80) **(b)** SE images, compatible with flow or dense calcification. **(c)** On axial GRE (150/15) image obtained with 50° flip angle, more profound hypointensity (arrows) in areas of signal void on SE images is compatible with CT-documented calcification, not flow, in patent vessels.

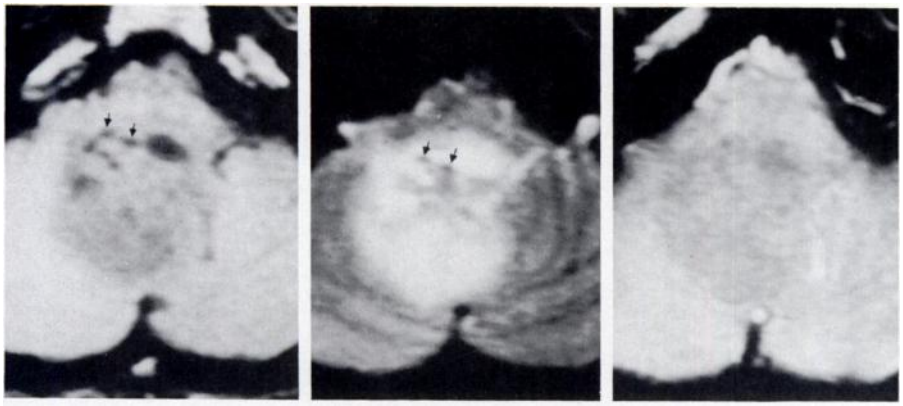

a. b. c.

Figure 11. MR images of avascular astrocytoma. On CT scans, large posterior fossa mass showed marked enhancement consistent with hemangioblastoma. On axial short TR/TE (600/20) **(a)** and long TR/TE (2,500/80) **(b)** SE images, lesion contains focal and irregular areas of hypointensity (arrows), possibly indicating extensive vascularity. **(c)** On axial GRE (150/15) image obtained with 50° flip angle, absence of high intensity in regions that displayed hypointensity on SE images is consistent with operative findings of avascular astrocytoma rather than hemangioblastoma.

ent) is not section-selective. Therefore, spins that originally are in the appropriate section for the application of the excitation radio-frequency pulse can still contribute signal, even if they have moved out of that plane during the interpulse time (TE/2), assuming that they have not left the volume subject to the application of the read-out gradient. The nonselectivity of refocusing in GRE imaging does not result in hyperintensity of incoming spins; it merely gives flowing spins the same signal intensity as stationary spins (if all other factors are the same) rather than signal void.

3. Another component of GRE imaging that contributes to the high intensity displayed by blood flow is the introduction of gradient pulses for correction of phase changes due to flow. We used the technique of gradient moment nulling (3) to compensate for constant-velocity flow only (first-order motion). Rephasing induced by this method of flow compensation cannot result in higher signal intensity for blood flow than for stationary fluid of the same composition. Extra gradient pulses were added to the section-select and read-out gradients in our GRE acquisitions.

Our results indicate that the value of GRE imaging for vascular intracranial lesions is limited and often depends on the specific lesion in question. AVMs are usually easily diagnosable on the basis of the SE images alone. The enlarged vascular structures were clearly seen as signal void in the vast majority of cases on short TR/TE and long TR/TE images. The high intensity of cerebrospinal fluid on long TR/TE SE images often was very useful in highlighting lesions that contained regions of signal void, especially when the abnormal vessels were intraventricular or located over the convexities (Figs 1, 3). More subtle vascular lesions, such as small venous angiomas (Fig 8), may become more conspicuous on GRE images. In two patients who had undergone proton-beam radiation therapy for AVMs, GRE images allowed confident distinction between small regions of residual patent vascular channels and hypointensity of perilesional hemosiderin seen on SE images (Fig 2). Treated AVMs therefore may necessitate adjunctive GRE imaging emphasizing flow for complete noninvasive evaluation.

The appearance of large tumor vessels was more specific on GRE images. In these cases, the initial interpretation of hypointensity on SE images as due to vascular flow void was verified or disproved on the basis of the GRE images. For example, in a surgically proved, partially calcified ependymoma, the sensitivity of GRE acquisition to magnetic-susceptibility differences allowed a confident specific diagnosis of intratumoral calcification, rather than blood flow in vessels, as the cause of SE signal voids (Fig 10). In another case, a surgically proved avascular posterior fossa astrocytoma, thought initially to represent a hemangioblastoma on the basis of CT findings, was depicted as being without large vessels on the GRE image (Fig 11). Adjunctive GRE imaging of intracranial neoplasms for possible vascularity therefore seems to be another indication for this technique, both as a means of improving the specificity of MR imaging in brain tumors and perhaps as a means of assessing the degree of malignancy.

GRE imaging was often helpful in ascertaining whether ambiguous intravascular SE signal-intensity patterns represented patent or thrombosed lumina (Figs 12, 13). The diag-

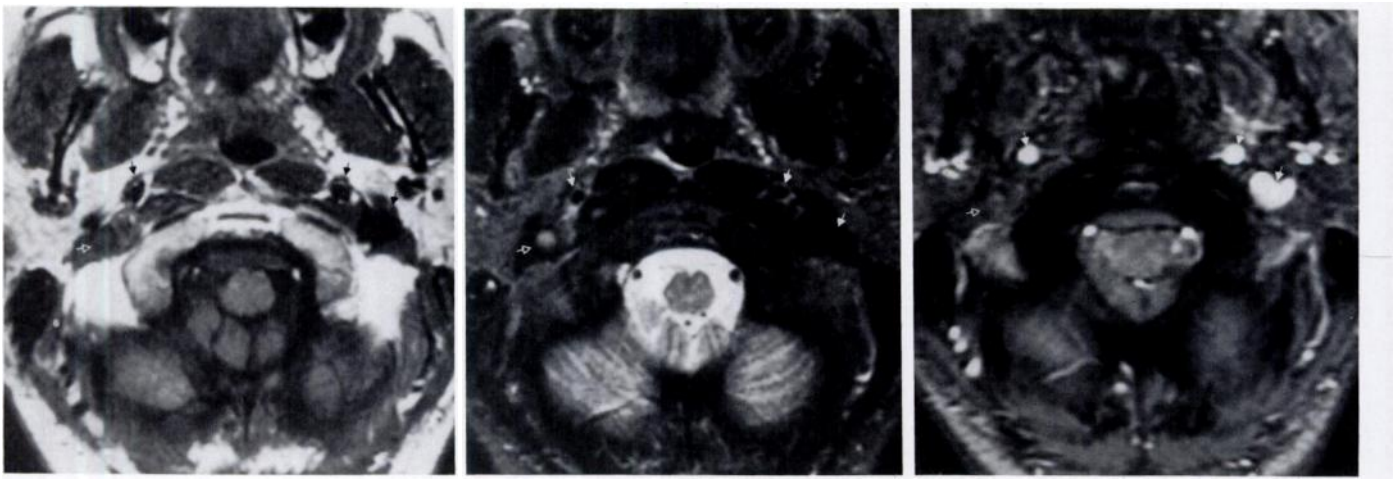

a. b. c.

Figure 12. MR images of thrombosed right internal jugular vein. Normal left internal jugular vein and left and right internal carotid arteries (closed arrows) all demonstrate signal void on axial short TR/TE (600/20) **(a)** and long TR/TE (2,800/80) **(b)** SE images. Right internal jugular vein (open arrow) shows moderate intensity on short TR/TE image **(a)** and increased intensity on long TR/TE image **(b)**, indicating either slow flow or thrombosis. **(c)** High-intensity patent vessels (closed arrows) and low-intensity thrombosed right internal jugular vein (open arrow) can be differentiated unambiguously on axial GRE (150/15) image obtained with 50° flip angle.

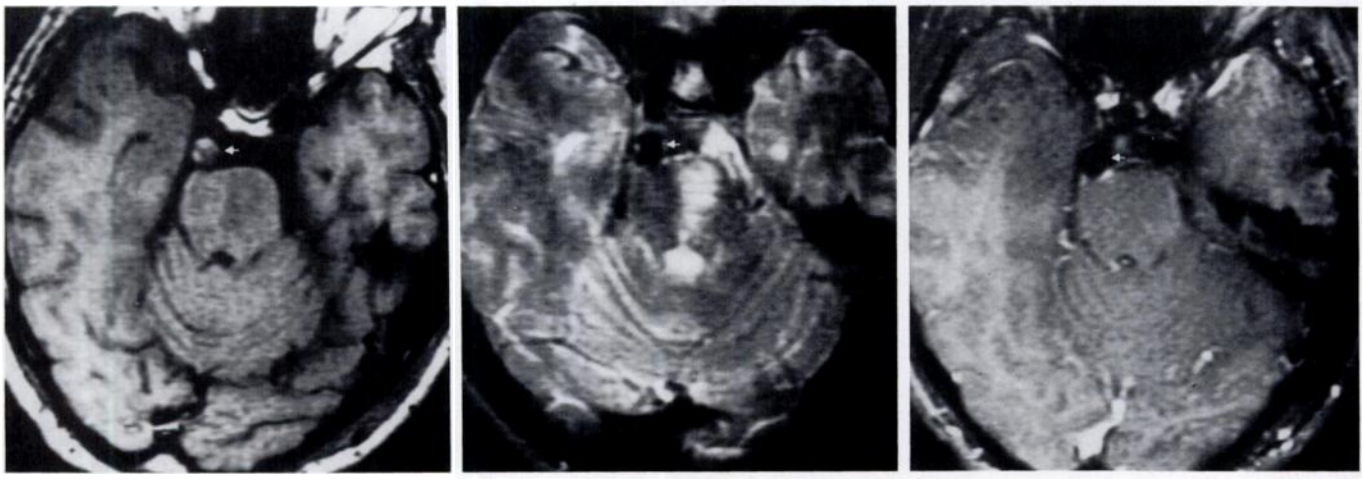

a. b. c.

Figure 13. MR images of thrombosed basilar artery (arrow). Ambiguous signal-intensity pattern seen in basilar artery on axial short TR/TE (600/20) **(a)** and long TR/TE (2,500/80) **(b)** SE images could indicate relatively slow flow or thrombosis. Left pontine infarction is clearly seen on both SE images. **(c)** Axial GRE (150/15) image obtained with 50° flip angle depicts definite low intensity in basilar artery, indicating thrombosis rather than slow flow.

nosis of vascular occlusion and the clarification of patency in partially thrombosed giant aneurysms were often possible on these images, due to the depiction of blood flow as high intensity. It has been clearly shown that certain SE sequences may depict vascular flow as variable intensities under certain conditions, mainly due to the phenomena of flow-related enhancement and even-echo rephasing (6,7). Furthermore, the recent implementation of flow-compensation techniques, such as gradient moment nulling (3), in routine head imaging (on long TR SE images) often results in high intensity within or adjacent to patent vessels.

There are several pitfalls in evaluating blood flow with this GRE technique. The major limitation of using GRE imaging to discriminate flow from thrombus lies in cases in which a hyperintense subacute clot of methemoglobin is present. Methemoglobin appears as high intensity on GRE images obtained with the use of imaging variables (relatively large flip angle and short TE) selected to demonstrate flow as high intensity (Fig 9), since the contrast in these images is relatively T1 dependent (4). Furthermore, even though flow may be present, GRE images can still demonstrate low intensity in certain cases. When GRE images are obtained without gradient moment nulling (or with inadequate compensation for higher-order flow effects), flow is not consistently depicted as high intensity, even though other imaging variables are unchanged (Fig 5). Turbulent flow is also seen as low intensity due to irretrievable random spin dephasing (8); in approximately one-third of the AVMs in our series, substantial areas of patency were depicted as low intensity on GRE images, presumably due to turbulence (Fig 3). In-plane flow and extremely slow flow (5,9) can theoretically be manifest as low intensity on GRE images, although in practice these have not been problematic in our experience.

Hemorrhagic complications of vascular lesions are often more obvious on GRE images. This heightened sensitivity of GRE imaging to blood-breakdown products has been report-

Table 1
Uses of GRE Imaging in Vascular Intracranial Lesions

Small vascular malformations with abnormal flow
Venous angiomas
Residual AVMs after therapy
Vascular malformations without abnormal flow (eg, cavernous hemangiomas)
Neoplasm characterization
Differentiating blood flow from calcification
Differentiating blood flow from hemosiderin
Intravascular thrombosis (except when subacute clot is present)
Hemorrhagic complications of vascular lesions

ed by many investigators (10–12) and is due to local magnetic-susceptibility differences from paramagnetic evolutionary stages of hemorrhage. These susceptibility changes result in the static local magnetic field perturbations that shorten T2*, an effect that is compensated for by the 180° radiofrequency pulse used in SE imaging. Therefore, hemorrhage from an AVM or a hemorrhagic occult cerebrovascular malformation can be seen on GRE images when the SE images fail to depict the lesion (Fig 6). In one of our cases, however, an AVM was partly obscured on the GRE image by a diamagnetic susceptibility gradient-induced hypointensity artifact due to its proximity to air-brain interfaces (Fig 4). It should be noted that the hypointensity from T2* effects seen on GRE images can be associated with both acute and chronic hemorrhage. Furthermore, this appearance is not specific for intracellular blood by-products, since calcification (13), turbulent flow (8), chemical shift, and the boundary of regions differing in magnetic susceptibility (10) all are associated with hypointensity on GRE images.

In summary, GRE images can be rapidly obtained to successfully demonstrate blood flow in vascular intracranial lesions as high signal intensity. In most cases, however, SE images clearly demonstrate the vascular nature of these lesions by the presence of signal void. In a limited number of cases (Table 1), such as treated AVMs and small vascular malformations with an equivocal appearance on the SE examination, the GRE technique can clarify the vascular nature of the area in question. Other useful applications of this technique include the diagnosis of hemorrhagic complications of vascular lesions, the detection of occult cerebrovascular malformations and large-vessel thrombosis (unless the clot is in the high-intensity methemoglobin stage), and characterization of intracranial neoplasms visualized as heterogeneous signal loss on SE images. ■

References

1. Haase A, Frahm J, Matthaei D, et al. FLASH imaging: rapid NMR imaging using low flip angle pulses. J Magn Reson 1986; 67:258–266.
2. Wehrli F, Hecker Prost J, Roberts F. The distinguishing properties of gradient-recalled acquisition in the steady state (GRASS) (abstr). Magn Reson Imaging 1987; 5(suppl 1):105.
3. Pattany PM, Phillips JJ, Chiu LC, et al. Motion artifact suppression technique (MAST) for MR imaging. J Comput Assist Tomogr 1987; 11:369–377.
4. Buxton RB, Edelman RR, Rosen BR, et al. Contrast in rapid MR imaging: T1- and T2-weighted imaging. J Comput Assist Tomogr 1987; 11:7–16.
5. Fram E, Hedlund L, Dimick R, Glover G, Herfkens R. Parameters determining the signal of flowing fluid in gradient refocused imaging: flow velocity, TR and flip angle. In: Book of abstracts: Society of Magnetic Resonance in Medicine 1986. Vol 1. Berkeley, Calif: Society of Magnetic Resonance in Medicine, 1986; 84–85.
6. Bradley WG Jr, Waluch V. Blood flow: magnetic resonance imaging. Radiology 1985; 154:443–450.
7. Axel L. Blood flow effects in magnetic resonance imaging. AJR 1984; 143:1157–1166.
8. Evans A, Herfkens R, Spritzer CE, et al. The effects of turbulent flow on MRI signal intensity using gradient refocused echoes. In: Book of abstracts: Society of Magnetic Resonance in Medicine 1987. Vol 1. Berkeley, Calif: Society of Magnetic Resonance in Medicine, 1987; 354.
9. Fram E, Karis J, Evans A, et al. Fast imaging of CSF: the effect of CSF motion. In: Book of abstracts: Society of Magnetic Resonance in Medicine 1987. Vol 1. Berkeley, Calif: Society of Magnetic Resonance in Medicine, 1987; 314.
10. Edelman RR, Johnson K, Buxton R, et al. MR of hemorrhage: new approach. AJNR 1986; 7:751–756.
11. Mills TC, Ortendahl DA, Hylton NM, Crooks LE, Carlson JW, Kaufman L. Partial flip angle MR imaging. Radiology 1987; 162:531–539.
12. Atlas SW, Mark AS, Grossman RI, Gomori JM. Intracranial hemorrhage: gradient-echo MR imaging at 1.5 T—comparison with spin-echo imaging and clinical applications. Radiology 1988; 168:803–807.
13. Atlas SW, Grossman RI, Hackney DB, et al. Calcified intracranial lesions: detection with gradient echo acquisition rapid MR imaging. AJNR 1988; 9:253–259.